

# Kinetic dissociation of nickel titanate and nickel tungstate in oxygen potential gradients

D. C. AZUBIKE

*Alcan International Ltd., Banbury, Oxon, OX16 7SP, UK*

A. CHRYSANTHOU

*Department of Materials Engineering and Materials Design, University of Nottingham, Nottingham, NG7 2RD, UK*

B. S. TERRY

*Department of Materials, Imperial College, London, SW7 2BP, UK*

Nickel titanate ( $\text{NiTiO}_3$ ) and nickel tungstate ( $\text{NiWO}_4$ ) were exposed to oxygen potential gradients at 1400 and 1100 °C, and they were found to dissociate into their constituent oxides, namely, NiO and  $\text{TiO}_2$ , and  $\text{WO}_3$  and NiO, respectively. This is consistent with the non-equilibrium phenomenon of kinetic decomposition. In the case of nickel titanate, at the low-oxygen-potential side,  $\text{TiO}_2$  was formed as sharp needle-like structures within the titanate matrix, while at the high-oxygen-potential side, NiO was formed. In contrast, NiO was formed at the lower-oxygen-potential side in the case of nickel tungstate, while  $\text{WO}_3$  volatilized off from the high-oxygen-potential side. This indicated that W diffuses faster than Ni in tungstates. In both cases, there were significant macroscopic shifts of the oxide with respect to the original position, established with Pt markers, towards the high-oxygen-potential side.

## 1. Introduction

Multicomponent oxide minerals are important sources of such transition metals as chromium, niobium, titanium and tungsten. Common examples of these minerals include chromite ( $\text{FeCr}_2\text{O}_4$ ), columbite ( $\text{FeNb}_2\text{O}_6$ ), wolframite ( $\text{FeWO}_4$ ), scheelite ( $\text{CaWO}_4$ ), ilmenite ( $\text{FeTiO}_3$ ) and perovskite ( $\text{CaTiO}_3$ ). In general, multicomponent oxides are unstable at elevated temperatures in gradients of temperature, pressure and chemical potential; this instability arises from the differences in the relative mobilities of the atomic constituents [1-4]. The processing of these important strategic minerals, currently occurs at elevated temperatures, and the effects of generalized thermodynamic gradients on their beneficiation needs to be understood therefore.

Schmalzried and co-workers [1-5] were the first to explain the non-equilibrium phenomenon arising from the effect of oxygen potential gradients on semiconducting-oxide solids. They showed that homogeneous oxide solid solutions can exhibit demixing, and ternary compounds dissociate in oxygen potential gradients. They have also reported that the oxide crystal itself macroscopically shifted towards the higher oxygen potential with respect to its original position under certain thermodynamic conditions, a similar observation has been made for the single (pure) oxide CoO system [4]. Measurements were reported on the demixing of the (Mg, Co)O solid solution [1, 2], and the dissociation of cobalt and nickel titanates [2, 3], and fayallite and olivines [5], in

oxygen potential gradients. Recently, Wolfenstine *et al.* [6] and Jacob and Shukla [7] have independently reported on the kinetic dissociation in oxygen potential gradients of  $\text{Ni}_2\text{SiO}_4$ . Jacob [8] has found that  $\beta$ -alumina, a super-ionic conductor underwent decomposition to  $\text{Al}_2\text{O}_3$  and  $\text{NaAlO}_2$  at the electrodes in oxygen potential gradients during a free-electron-flow closed-circuit electrolysis.

It is interesting to note that the primary interest of the previous workers has centred on understanding the effects of thermodynamic gradients on multicomponent oxide ceramics with a view to utilizing them as structural materials at high temperatures. The main purpose of the work presented here is the use of the phenomenon of kinetic dissociation in facilitating the beneficiation of strategic metals from their complex oxide minerals and to examine the possible influence such dissociation behaviour may have on existing beneficiation processes. The ternary oxides chosen in the first instance were  $\text{NiTiO}_3$  and  $\text{NiWO}_4$  since there are thermodynamic data available and these oxides also avoid the problems associated with the multivalent nature of iron in analogous iron compounds (which better approximate real minerals of commercial interest). The conclusions reached regarding the role of kinetic dissociation in determining the nature of these phases should be of fundamental importance in the high-temperature processing of oxide materials. Therefore, the work presented here represents a preliminary report on the role of kinetic dissociation in the beneficiation of complex oxides.

## 2. Experimental procedure

The apparatus is shown schematically in Fig. 1. The furnace had a vertically positioned alumina tube with platinum windings, and its temperature was controlled by means of a Eurotherm regulator using a Pt/Pt-13% Rh thermocouple. The reaction tube was made of either alumina or recrystallized silica depending on the experimental temperature.

The nickel titanate was prepared from stoichiometric amounts of nickel oxide and titania. An intimate mixture of both compounds was initially heated at 1200 °C for 24 h. After cooling to room temperature the mixture was ground, pelletized and homogenized at 1100 °C for 3 days. Nickel tungstate was prepared by precipitation from aqueous solutions of sodium tungstate and nickel sulphate. The oxide precipitate was repeatedly washed with distilled water to remove any adhering excess solution, it was dried in air at

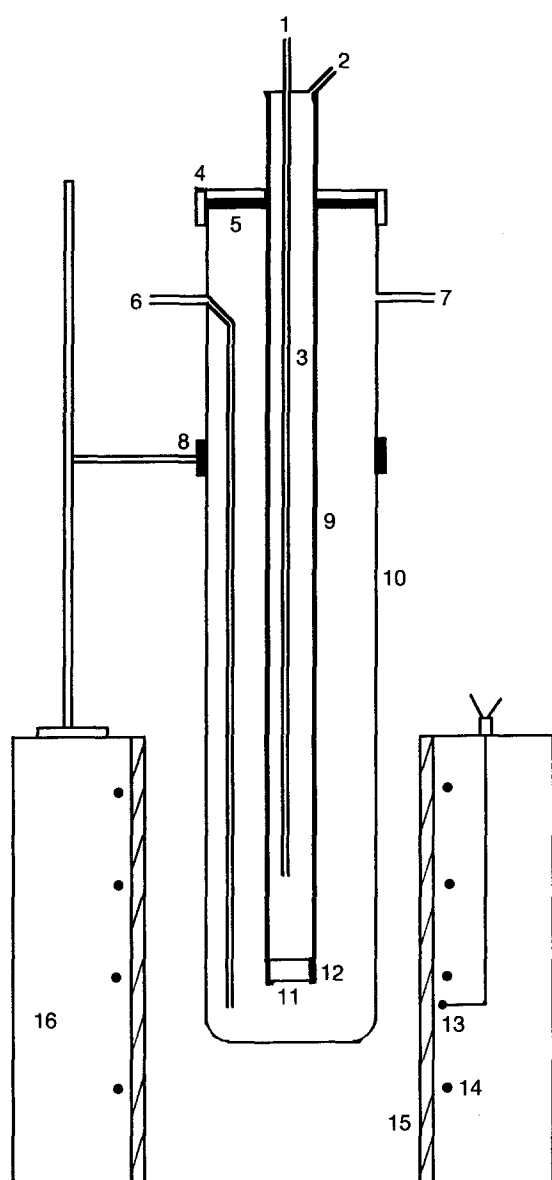


Figure 1 Apparatus for placing an oxide sample in an oxygen potential gradient: (1) CO/CO<sub>2</sub> inlet, (2) CO/CO<sub>2</sub> outlet, (3) narrow alumina tube, (4) plastic screw cap, (5) O-ring seal, (6) air inlet, (7) air outlet, (8) retort clamp, (9) mullite tube, (10) reaction tube, (11) oxide sample, (12) Pt foil, (13) thermocouple, (14) Pt windings, (15) furnace alumina tube, (16) alumina insulation.

150 °C for 20 h and then heat treated at 700 °C for 24 h. In both cases, X-ray diffraction (XRD) was used to confirm the presence of a single phase.

Samples were prepared by hot pressing finely ground oxide powder of known weight at 1100 °C and 40 MPa pressure in a 10 mm alumina die to give a sample thickness of less than 3 mm, and ~95% of theoretical density. The pellets were then polished to produce flat parallel surfaces. The cylindrical sides of the oxide pellet were wrapped in Pt foil. The pellet was then stuck to one end of a mullite tube using Pt paste (which also served as a position marker), by heating at 800 °C for 6 h in order to obtain a hermetic seal.

For all experiments the oxygen potential gradient was that of air ( $P'_{O_2} = 0.213$ ) and the low oxygen potentials were established by varying the CO/CO<sub>2</sub> ratio, using the appropriate thermodynamic data [9] for the reaction  $CO + \frac{1}{2}O_2 = CO_2$ . After completion of each experiment, the pellet was sectioned parallel to the diffusion direction, mounted in araldite and polished with diamond lapping compounds. Optical micrographs were obtained using a Reichert microscope, while steady-state concentration profiles were determined on a JEOL-35 electron microscope.

## 3. Results

The results of the dissociation experiments performed on nickel titanate and nickel tungstate are summarized in Table 1. Fig. 2 shows the results of the decomposition experiment B and substantiates the work of Laqua and Schmalzried [3]. The NiTiO<sub>3</sub> sample was held in an oxygen potential gradient with  $P''_{O_2}/P'_{O_2} = 2940$ . It should be stressed here that NiTiO<sub>3</sub> is stable at both the oxygen potentials applied, with the lower potential being 7.2 Pa. In the presence of a gradient it decomposed into NiO (TiO<sub>2</sub>-saturated) at the high-oxygen-potential side and TiO<sub>2</sub> at the lower-oxygen-potential side.

The decomposed phases were not clearly demarcated from one another due to morphological instability

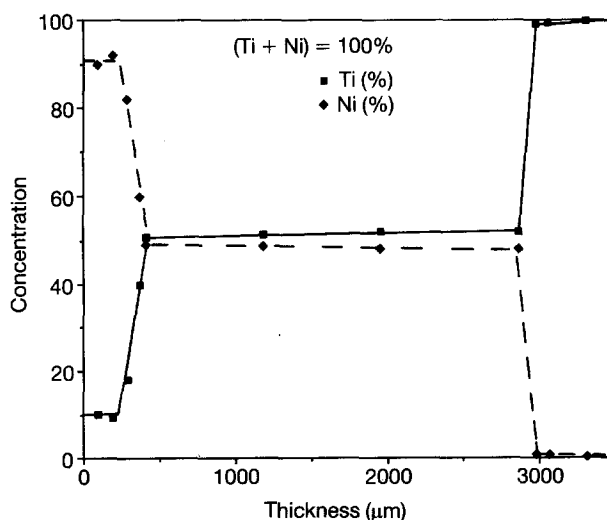


Figure 2 Multiphase layer formed by exposing a single-phase NiTiO<sub>3</sub> to an oxygen potential gradient between  $2.13 \times 10^4$  Pa and 7.234 Pa at 1450 °C (Experiment B).

TABLE I Coexisting phases formed after attaining steady-state conditions  $P''_{O_2} = 2.13 \times 10^4$  Pa

| Experiment                  | $P''_{O_2}/P'_{O_2}$ | Duration (h) | Temperature (°C) | Phase formed (thickness at end of experiment) ( $\mu\text{m}$ ) |   |                          |
|-----------------------------|----------------------|--------------|------------------|---|---|--------------------------|
| <i>a</i> NiTiO <sub>3</sub> |                      |              |                  |   |   |                          |
| A                           | 7300                 | 214          | 1350             | NiO (120)   | NiTiO <sub>3</sub> (3240)                 | TiO <sub>2</sub> (220)   |
| B                           | 2940                 | 240          | 1450             | NiO (335)   | NiTiO <sub>3</sub> (2620)                 | TiO <sub>2</sub> (530)   |
| C                           | 8250                 | 50           | 1350             | NiO (30)  | NiTiO <sub>3</sub> (2650)                 | TiO <sub>2</sub> (Trace) |
| <i>p</i> NiWO <sub>4</sub>  |                      |              |                  |   |   |                          |
| D                           | $4 \times 10^8$      | 140          | 1010             | NiO (80)  | NiWO <sub>4</sub> (3400)                  | WO <sub>3</sub> (Trace)  |
| E                           | $1.7 \times 10^8$    | 80           | 1050             | –   | NiWO <sub>4</sub> (3500)<br>(no demixing) | –                        |
| F                           | $1.1 \times 10^7$    | 50           | 1110             | –   | NiWO <sub>4</sub> (4500)                  | –                        |

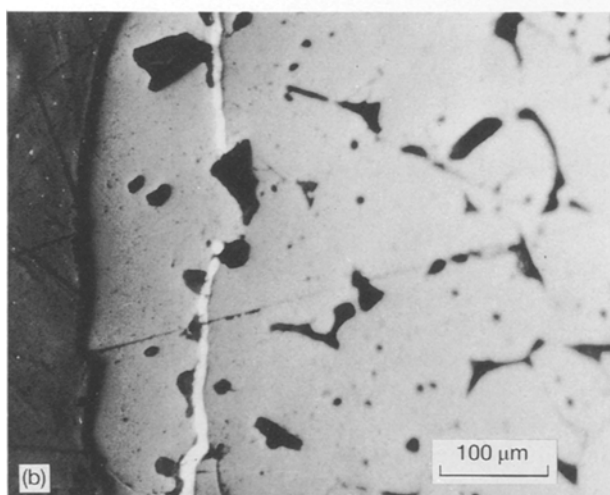
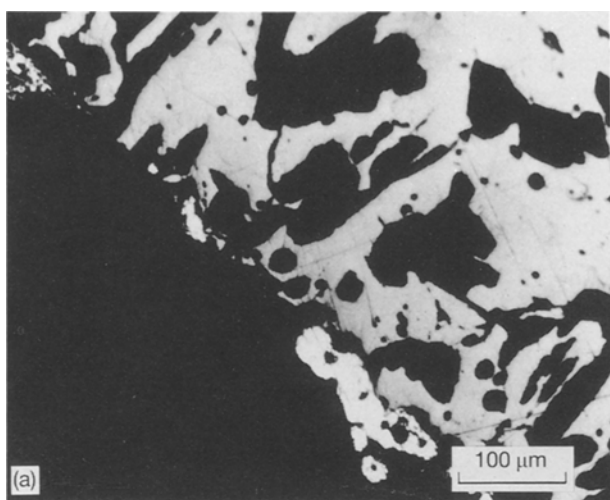


Figure 3 Optical micrographs of dissociated nickel titanate. (a) low oxygen potential side, (b) high oxygen potential side. (Pt-markers are the white phase.)

especially near the low-oxygen-potential surface. The thickness of each phase given in Table I is therefore estimated as being equal to the mean of the distance at which the phase just starts to contain traces of the adjoining phases and the distance where the phase

disappears completely, these distances being obtained from sample-concentration profiles and optical-microscopy measurements.

Fig. 3 presents optical micrographs of the dissociated NiTiO<sub>3</sub> sample, Fig. 3a being at the low-oxygen-potential side, where the crystal has moved away from the Pt marker (white regions). A large region of voids and pores (black) was observed depicting the morphological instability of this interface. On the high-potential-side, Fig. 3b, the grey NiO phase has moved past and Pt marker (white), emphasizing the overall macroscopic shift of the crystal.

Fig. 4 is a scanning electron micrograph from the low oxygen-potential side of the sample. In contrast to the results of Schmalzried and Laqua [2, 3] this micrograph shows sharp needle-like precipitates of TiO<sub>2</sub> which are  $\sim 2 \mu\text{m}$  thick, nucleating near pore edges and growing into the NiTiO<sub>3</sub> matrix.

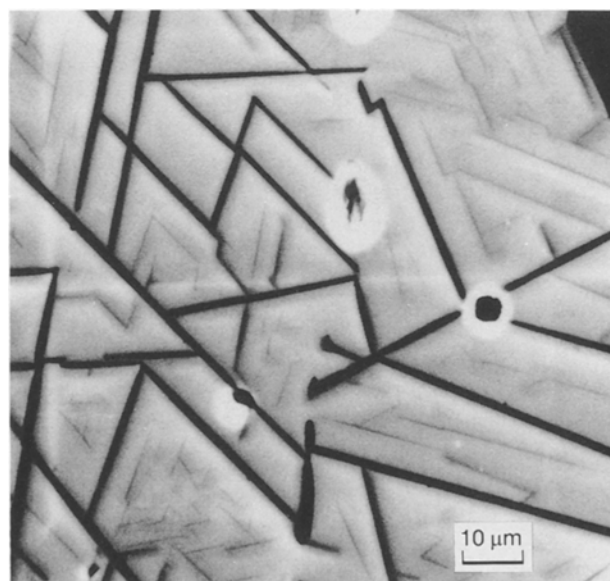
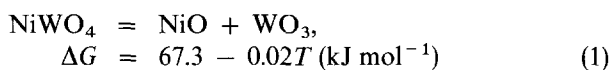


Figure 4 Electron micrograph of the low oxygen potential side of NiTiO<sub>3</sub> crystal exposed to an oxygen potential gradient at 1450 °C ( $P''_{O_2} = 0.213 \times 10^4$  Pa,  $P''_{O_2}/P'_{O_2} = 2940$ ).

In the case of  $\text{NiWO}_4$ , which is the only stable ternary phase in the Ni–W–O system [10], the concentration profiles on the electron microscope showed the presence of two phases, NiO and  $\text{NiWO}_4$ , the nickel oxide being detected at the low-oxygen potential side. The interface near the high-oxygen-potential side was found to be almost nearly as morphologically unstable (that is full of pores and fissures) as that near the low-oxygen-potential side. An important aspect of the observed decomposition is the physical separation of the product phases.

#### 4. Discussion

The free energy for the dissociation reaction of  $\text{NiWO}_4$  is given by



and the oxygen partial pressure at  $1010^\circ\text{C}$  corresponding to NiO dissociation is  $1.72 \times 10^{-9}$  Pa. The oxygen partial pressures used in this investigation were above this dissociation pressure by a factor of at least ten, therefore, chemical decomposition of  $\text{NiWO}_4$  was not expected under these experimental conditions.

Atomic species in an ionic crystal can move under the action of electrochemical potential gradients. In transition-metal oxides (local) the level of equilibrium cationic vacancies or the interstitial concentration depend on the oxygen potential. The exact functional dependence is determined by the dominant point defects present in the system. When an isothermal oxygen potential gradient is imposed on  $\text{NiWO}_4$  it induces a vacancy gradient in the cationic sublattices. As a result of this gradient, cations are transported to the oxide surface exposed to the higher oxygen potential with coupled transport of electron holes in the opposite direction. If the mobility of one of the cationic species in the multicomponent oxide is higher than that of the others, there is a preferential flux of that species until a steady state is attained. Laqua and Schmalzried [3] have developed quantitative mathematical relations for the critical oxygen potential gradients required to initiate decomposition and the steady-state crystal velocity. A summary shall be given, using the direction of fluxes and sample movement indicated in Fig. 5.

From linear transport theory, the flux of an atomic specie such as  $\text{Ni}^{2+}$  under a potential gradient in

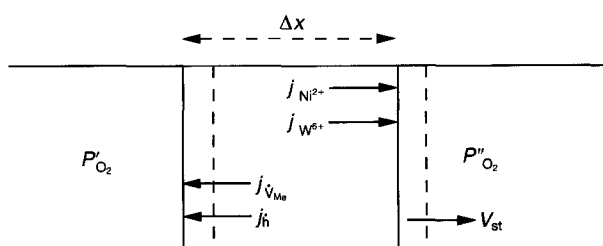


Figure 5 A schematic plot of the fluxes of cations, vacancies and electron holes within a  $\text{NiWO}_4$  crystal in an oxygen potential gradient.

a particular direction ( $x$ ) is given by

$$J_{\text{Ni}^{2+}} = - \frac{C_{\text{Ni}} D_{\text{Ni}}}{RT} \frac{\delta \eta_{\text{Ni}^{2+}}}{\delta x} \quad (2)$$

where the driving force is the electrochemical potential,  $\eta_{\text{Ni}^{2+}}$ , comprising of a chemical term ( $\mu_{\text{Ni}^{2+}}$ ) and an electrical field contribution ( $Z_{\text{Ni}^{2+}} F \phi$ ), where  $Z$  is the atomic charge,  $F$  is the Faraday constant and  $\phi$  is the electric potential.  $C_{\text{Ni}}$  and  $D_{\text{Ni}}$ , respectively, denote the concentration (in moles per unit volume) and diffusion coefficient of nickel ions in the tungstate. In general, diffusivities of cations in multicomponent oxides are not only functions of total pressure and temperature, but also vary with chemical potentials, so in this treatment only average coefficients can effectively be used.

Applying the principle of local equilibrium, the chemical potentials of ionic species can be written in terms of chemical potentials of neutral species and electronic defects as follows



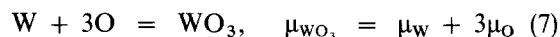
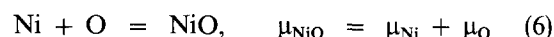
where  $h \cdot$  is an electron hole.  $\text{NiWO}_4$  is a semiconductor thus  $-dF\phi = d\mu_{h \cdot}$ , therefore

$$J_{\text{Ni}} = - \frac{C_{\text{Ni}} D_{\text{Ni}}}{RT} \frac{\delta \mu_{\text{Ni}}}{\delta x} \quad (4)$$

Similarly, the flux for tungsten is

$$J_{\text{W}} = - \frac{C_{\text{W}} D_{\text{W}}}{RT} \frac{\delta \mu_{\text{W}}}{\delta x} \quad (5)$$

From the equilibrium conditions for the formation of the binary oxides, the following equations can be written



Combining Equations 4 and 6

$$J_{\text{Ni}} = - \frac{C_{\text{Ni}} D_{\text{Ni}}}{RT} \left( \frac{\delta \mu_{\text{NiO}}}{\delta x} - \frac{\delta \mu_{\text{O}}}{\delta x} \right) \quad (8)$$

and similarly

$$J_{\text{W}} = - \frac{C_{\text{W}} D_{\text{W}}}{RT} \left( \frac{\delta \mu_{\text{WO}_3}}{\delta x} - 3 \frac{\delta \mu_{\text{O}}}{\delta x} \right) \quad (9)$$

In the steady state no further decomposition occurs, and all species move with the same velocity,  $V_{\text{st}}$ , hence

$$V_{\text{st}} = \frac{J_{\text{Ni}}}{C_{\text{Ni}}} = \frac{J_{\text{W}}}{C_{\text{W}}} \quad (10)$$

Substituting for the fluxes in Equation 10, we obtain

$$D_{\text{Ni}} \frac{\delta(\mu_{\text{NiO}} - \mu_{\text{O}})}{\delta x} = D_{\text{W}} \frac{\delta(\mu_{\text{WO}_3} - 3\mu_{\text{O}})}{\delta x} \quad (11)$$

The Gibbs–Duhem equation for stoichiometric tungstate composition, that is,  $N_{\text{NiO}} = N_{\text{WO}_3}$  is

$$N_{\text{NiO}} d\mu_{\text{NiO}} + N_{\text{WO}_3} d\mu_{\text{WO}_3} = 0 \quad (12)$$

therefore

$$\frac{\delta \mu_{\text{WO}_3}}{\delta x} = - \frac{\delta \mu_{\text{NiO}}}{\delta x} \quad (13)$$

Substituting into Equation 12 and rearranging

$$\frac{\delta\mu_{\text{WO}_3}}{\delta x} = \frac{3D_{\text{W}} - D_{\text{Ni}}}{D_{\text{W}} + D_{\text{Ni}}} \frac{\delta\mu_{\text{O}}}{\delta x} \quad (14)$$

Integrating over the length of the crystal,  $\Delta x$

$$\Delta\mu_{\text{WO}_3} = \frac{3\beta - 1}{\beta + 1} \Delta\mu_{\text{O}} \quad (15)$$

where  $\beta = D_{\text{W}}/D_{\text{Ni}}$ , the mean values of the diffusion coefficients in the tungstate, and  $\Delta\mu_{\text{WO}_3}$  and  $\Delta\mu_{\text{O}}$  are the chemical potential differences of  $\text{WO}_3$  and O, respectively, at the ends of the crystal.

The maximum value of  $\Delta\mu_{\text{WO}_3}$  is dependent on the free energy of formation of  $\text{NiWO}_4$  assuming mutual insolubility between NiO and  $\text{WO}_3$ . Replacing  $\Delta\mu_{\text{O}}$  by oxygen partial pressures, we obtain

$$\ln(P''_{\text{O}_2}/P'_{\text{O}_2}) = 2 \frac{(\beta + 1)(-\Delta G)}{(\beta - 1)RT} \quad (16)$$

From Equation 16 it would appear that nickel ions diffuse faster than tungsten since the minimum ratio of diffusivities  $\beta$  required to cause dissociation is  $\frac{1}{3}$ . However, our experimental results show that NiO is found at the lower-oxygen-potential side and that tungsten ions migrated faster than nickel ions to form tungsten oxide at the higher-oxygen-potential side from where it has probably sublimated. This type of behaviour has been observed in the reverse phenomenon of the high-temperature oxidation of metal alloys. In the case of nickel-chromium alloys, one should expect the chromium, whose oxides gives the passivation (resistance) to oxidation, to migrate faster than nickel [11]. However, nickel oxide is always observed to form first, since here the nickel ions diffuse faster than chromium ions. Therefore, it is possible that in nickel tungstate, tungsten ions diffuse faster than nickel ions, and this behaviour can become useful in the beneficiation of complex tungsten-oxide minerals.

There are no independent experimental data for  $\beta$  (the ratio of diffusivities in nickel tungstate) confirm the above. However, using a ratio of oxygen partial pressures of  $4 \times 10^8$  at which dissociation was observed, and a free energy of formation of  $\sim 11 \text{ kcal mol}^{-1}$  at  $1010^\circ\text{C}$  [9, 10],  $\beta$  has been estimated to be 0.56, suggesting that nickel diffuses faster than tungsten and that no dissociation should occur under these conditions. However, it is important to note that the true ratio could be significantly different, since the length of the crystal is not constant throughout the experiment. Also, the oxygen potential difference increases with time due to the sublimation of  $\text{WO}_3$  and the increased fissures/pores at both oxygen-potential sides. The morphological instability observed unexpectedly at the high-potential side reinforces the view that there is  $\text{WO}_3$  phase sublimation on this side of the crystal. Clearly such a sublimation can have a profound effect on any analysis of possible kinetic dissociation effects. The results and analysis conducted with nickel tungstate must therefore be treated with caution.

A similar mathematical treatment using analogous assumptions has been made for  $\text{NiTiO}_3$  [2, 3]. The relationship between the ratio of partial pressures to the ratio of diffusivities of nickel and titanium in nickel titanate,  $\gamma$ , required to cause its dissociation is given as:

$$\ln(P''_{\text{O}_2}/P'_{\text{O}_2}) = 2 \frac{\gamma + 1}{\gamma - 2} \frac{(-\Delta G)}{RT} \quad (17)$$

where  $\gamma = D_{\text{Ni}}/D_{\text{Ti}}$  and  $\Delta G$  is the free energy of formation of  $\text{NiTiO}_3$ .

Our results show that  $\text{NiTiO}_3$  does dissociate into its constituent phases as expected, though the ratio of oxygen partial pressures used were at least 500 times greater than the minimum ratio predicted and experimentally observed by Laqua and Schmalzried [3]. However, in contrast we have observed that needle-like precipitates of  $\text{TiO}_2$  nucleated near pores at the low-oxygen-potential side at higher temperatures,  $\sim 1450^\circ\text{C}$ . It is possible that the combination of high temperatures and kinetic dissociation causes a change in the stoichiometry of the product phases.

Rewriting Equations 4 and 10 for  $\text{NiTiO}_3$  allows an evaluation of its steady velocity in terms of the crystal thickness and ionic diffusivities, as

$$J_{\text{Ni}} = - \frac{C_{\text{Ni}} D_{\text{Ni}}}{RT} \frac{\delta\mu_{\text{Ni}}}{\delta x} \quad (18)$$

and

$$d\mu_{\text{NiO}} = \frac{D_{\text{Ni}} - 2D_{\text{Ti}}}{D_{\text{Ni}} + D_{\text{Ti}}} d\mu_{\text{O}} \quad (19)$$

and hence

$$V_{\text{st}} = \frac{3D_{\text{Ti}} \ln(P''_{\text{O}_2}/P'_{\text{O}_2})}{4(\gamma + 1)\Delta x} \quad (20)$$

where  $\gamma = D_{\text{Ni}}/D_{\text{Ti}}$ , the ratio of diffusivities.

An approximation of the steady-state velocity can be obtained from the values of the thicknesses and experimental duration given in Table I for  $\text{NiTiO}_3$ . Using the ratio of diffusivities,  $\gamma$ , of 7.88 given in [3], the values calculated for  $D_{\text{Ti}}$  are between  $2 \times 10^{-9}$  and  $8 \times 10^{-10} \text{ cm}^2/\text{s}^{-1}$ , and these values are consistent with those reported for diffusion in similar ilmenite-type structures [12].

Our calculated values of  $\gamma$ , the ratio of the diffusivities of nickel and titanium in nickel titanate using  $\Delta G_{\text{NiTiO}_3} = -4300 + 2.0T$  [9] is 2.23 which is much smaller than that estimated by Laqua and Schmalzried [3]. However, it should be noted that no account has been taken of the activity contribution due to the miscibility of NiO in  $\text{NiTiO}_3$  and the lower free energy of formation  $\Delta G$ -values used in our calculations.

The oxygen potential gradient responsible for kinetic dissociation have been deliberately applied in the present study by the use of controlled-composition gas mixtures. The possibility also exists that such oxygen potential gradients can be established either inadvertently or by deliberate formation during the reduction of complex oxides. For example, the local reduction of one component to its elemental state provides the opportunity for the establishment of local oxygen potential gradients and may thus lead to kinetic dissociation becoming involved in the reduction process.

Similar phenomena can be clearly envisaged for the reduction of complex sulphide and arsenide minerals.

## 5. Conclusion

Nickel titanate and nickel tungstate have been kinetically dissociated into their constituent oxides in oxygen potential gradients. This decomposition is due to unequal rates of migrations of the cations within these oxides. Although, the kinetics involved here are very slow, the kinetic decomposition phenomena can contribute to improved materials processing, for example in the controlled *in-situ* formation of the reinforcing second phase in ceramic-matrix components or in the beneficiation of complex transition-metal-oxide minerals.

## Acknowledgements

The financial support from the SERC and the Association of Commonwealth Universities is gratefully acknowledged.

## References

1. H. SCHMALZRIED, W. LAQUA and P. LIN, *Z. Naturforsch* **A34** (1979) 192.
2. *Idem*, *Oxid. Met.* **15** (1981) 339.
3. W. LAQUA and H. SCHMALZRIED, in "Chemical metallurgy – a tribute to Carl Wagner" (The Minerals, Metals and Materials Society-American Institute of Mining, Metallurgy and Petroleum Engineers, 1981) p. 29.
4. G. J. YUREK and H. SCHMALZRIED, *Ber. Busenges. Physik. Chem.* **79** (1975) 255.
5. R. WEGHOFT and H. SCHMALZRIED, *Mater. Sci. Forum* **7** (1986) 223.
6. J. WOLFENSTINE, D. DIMOS and D. L. KOHLSTEDT, *J. Amer. Ceram. Soc.* **68** (1985) C117.
7. K. T. JACOB and A. K. SHUKLA, *J. Mater. Res.* **2** (1987) 338.
8. K. T. JACOB, *J. Appl. Electrochem.* **13** (1983) 469.
9. E. T. TURKDOGAN, "Physical chemistry of high temperature technology", (Academic Press, London, New York, 1980) p. 5.
10. K. J. JACOB, *J. Mater. Sci.* **12** (1977) 1647.
11. G. Y. LAI, "High-temperature corrosion of engineering alloys", (American Society for Metals, Metals Park, Ohio, (1990) p. 15.
12. R. DIECKMANN, *Solid State Ionics* **12** (1984) 1.

*Received 25 March  
and accepted 8 October 1993*